

# Sol-gel preparation and thermo-mechanical properties of porous $x\text{Al}_2\text{O}_3-y\text{SiO}_2$ coatings on SiC Hi-Nicalon fibres

Martine Verdenelli, Stephane Parola\*, Fernand Chassagneux, Jean-Marie Létoffé, Henri Vincent, Jean-Pierre Scharff, Jean Bouix

*Laboratoire des Multimatériaux et Interfaces UMR CNRS 5615, Université Claude Bernard Lyon 1, 69622 Villeurbanne cedex, France*

Received 15 June 2002; received in revised form 30 August 2002; accepted 7 September 2002

## Abstract

Porous thin films of mixed aluminium silica oxides were elaborated by the sol-gel process from aluminium tri-sec-butoxide and tetraethylorthosilicate on Hi-Nicalon fibres. The porosity was generated by addition of a surfactant, namely cetyltrimethylammonium bromide (CTAB). SiC Hi-Nicalon fibres were coated by the dip-coating technique. After annealing in air (500–1200 °C) crack-free coatings were observed, with a thickness in the range 100–1000 nm. The fibres were tensile tested and results were analysed by the Weibull statistic. They showed good mechanical properties compared to the commercial fibres. The systems were characterized by thermal gravimetry, differential scanning calorimetry, X-ray diffraction, BET and scanning electron microscopy. The powders obtained in the same conditions as the coatings were highly porous with surface areas in the range 540–150 m<sup>2</sup>/g depending on the annealing temperature (400–1000 °C).

© 2002 Elsevier Science Ltd. All rights reserved.

*Keywords:* Al<sub>2</sub>O<sub>3</sub>; Composites; Porosity; SiC fibres; Sol-gel processes; SiO<sub>2</sub>

## 1. Introduction

Fibre-reinforced ceramic matrix composites (CMCs) are of great interest for applications under high thermal conditions or mechanical constraints (e.g. vehicles, aerospace). The concept of porous and/or oxide interphase for the deflection of matrix cracks has been known for several years (Fig. 1).<sup>1–5</sup> However, it has never been demonstrated whether a such interphase could work or not. More recently it was reported that oxide coatings can act as a diffusion barrier and provide, for example, suitable protection against oxidation or corrosion reactions.<sup>6–11</sup> In this work, the elaboration and characterization of oxide interphase with controlled porosity on Hi-Nicalon SiC fibres are reported together with their mechanical behavior.

Several methods can be used to elaborate thin films on fibres, including chemical vapour deposition (CVD), sputtering and the sol-gel process. Among the numerous advantages of the sol-gel process compared to conventional methods,<sup>12</sup> the low temperature and the possibility

of controlling the porosity by adding various templates were of a great interest for our purpose. Several templates can be used to create the porosity in the oxide, the chelating ligand acetylacetonate (acac<sup>-</sup>) and the ionic surfactant cetyltrimethylammonium bromide C<sub>16</sub>H<sub>33</sub>N(CH<sub>3</sub>)<sub>3</sub>Br (CTAB) for respectively micro- and meso-porosity are reported here. Silica doped alumina systems were selected for their high temperature of crystallization and melting, in order to maintain the porosity even at high temperature. Two binary mixtures are reported here, 3 Al<sub>2</sub>O<sub>3</sub>-2 SiO<sub>2</sub> (**1**) and a 10% (in weight) SiO<sub>2</sub> doped alumina (**2**), which, according to the equilibrium phase diagram should give respectively the mullite phase Al<sub>6</sub>Si<sub>2</sub>O<sub>13</sub>, and a solid solution  $x\text{Al}_2\text{O}_3-y\text{SiO}_2$  which leads to a mixture of two phases  $\alpha\text{-Al}_2\text{O}_3$  (corundum) and the mullite.

## 2. Experimental procedure

### 2.1. Sol preparation

All experiments were performed under an inert atmosphere using standard Schlenk techniques. 2-Propanol

\* Corresponding author. Tel.: +33-472-448-167; fax: +33-472-431-568.

*E-mail address:* stephane.parola@univ-lyon1.fr (S. Parola).

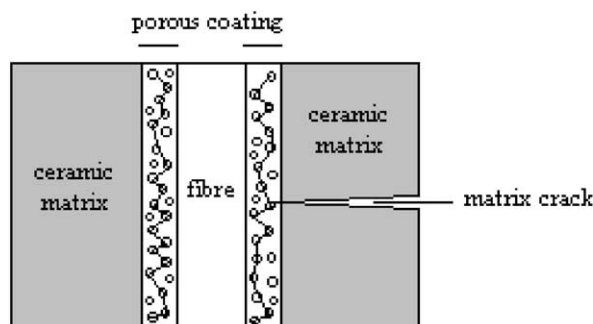


Fig. 1. The concept of porous interphase for the reinforcement of CMCs.

and aluminium tri-sec-butoxide (Aldrich) were distilled prior to use. Table 1 lists the compositions of the solutions of precursors. Aluminium tri-sec-butoxide, tetraethylorthosilicate (TEOS, Prolabo) and cetyltrimethylammonium bromide (CTAB, Aldrich) were dissolved separately in 2-propanol. The TEOS/2-propanol solution was then added to the aluminium precursor. Acetylacetonate (Aldrich) which act as chelating ligand<sup>13–16</sup> was used to stabilize the aluminium precursor towards hydrolysis reactions<sup>17,18</sup> and to create the micro-porosity. The calculated volume of the CTAB solution was then added. The resulting solution was stirred for one hour to obtain the Al/Si/O solution used for the coating. The solutions were filtered with 1  $\mu\text{m}$  filters prior to deposition.

### 2.2. Powders elaboration and sol-gel coatings of SiC fibres

The powders used for the BET measurements and powder X-ray diffraction were prepared by complete hydrolysis of the solutions of precursors with a ratio  $h=20$  ( $h=[\text{H}_2\text{O}]/[\text{M}(\text{OR})_n]$ ), filtration, drying and thermal annealing of the powder.

The Hi-Nicalon SiC fibres, manufactured by Nippon Carbon (Japan) were selected as substrate. Commercial fibres were desized for 30 min in air at 600 °C before deposition. This treatment creates a thermally evolved SiO<sub>2</sub> coating to enhance the adhesion of the sol-gel coating. The single fibres were mounted on a specific support before deposition and dip-coated in the solution of precursors, maintained for 5 min and drawn out vertically with a withdrawal speed of 300 mm. min<sup>-1</sup>. Thermal treatments were optimized in order to obtain

Table 1  
Compositions of the solutions (mol) used for the deposition of the porous oxides

Sample	Al(OBu <sup>s</sup> ) <sub>3</sub>	Si(OEt) <sub>4</sub>	acacH	CTAB
1	6	2	6	1.5
2	1	0.095	1	0.25

crack free coatings. The coatings were slowly heated at about 120 °C to eliminate the solvent. Multilayered films were obtained by repeating those operations. The best quality for the films was obtained when three layers were deposited. Finally, annealing of the samples between 200 and 1200 °C were performed in air. During the final thermal treatments, the temperature was raised at a rate of 5 °C/min and the fibres were heated for 2 h before slowly cooling down to room temperature.

### 2.3. Characterization

Thermogravimetric analysis (TGA) was carried out using a Mettler-Toledo TGA/SDTA/851<sup>c</sup>. DSC measurements were performed with a Mettler-Toledo DSC 820. A TMA/SDTA 840 Mettler Toledo system was used for Thermomechanical analysis. All TGA, DSC and TMA experiments were carried out in the air. For phase analysis by X-ray powder diffraction (XRD), a standard Philips PW 1840 diffractometer with CuK $\alpha_1$  was used. Data were collected by step-scanning from 10 to 70° ( $2\theta$ ) with a step size of 0.020° ( $2\theta$ ) and 1 s counting time at each step. Specific surface areas were determined by the BET method at 77 K using N<sub>2</sub> as adsorptive agent. The morphology of the coated fibres was observed with a scanning electron microscope (SEM, Hitachi S800, 15 kV). The cross sections of the samples were prepared by cutting coated fibres with a sharp edge. The tensile strengths of the monofilaments were measured with an Adamel DY22 testing machine. The crosshead speed was 0.1 mm min<sup>-1</sup>, the load cell was 500 cN and the gauge lengths were 10 mm. Fifty monofilaments were tested for each sample. Before mechanical testing, the monofilament diameter was determined by laser interferometry. The results of the tensile tests were analysed by the Weibull statistic.<sup>19</sup>

## 3. Results and discussion

### 3.1. Elaboration of the films on the SiC fibres

The coatings of the fibres were performed using dip-coating technique. The starting materials for the oxides were metal alkoxides, namely aluminium tri-sec butoxide and TEOS (tetraethylorthosilicate). The precursors were mixed with a molar ratio of Al:Si = 3:1 or 10.5:1.

The aluminium and silicon precursors do not behave the same way toward hydrolysis reactions. Aluminium alkoxide are very easily hydrolysable while silicon alkoxides necessitate acid or basic conditions. An alternative in order to prepare a solution with precursors having a more similar reactivity is to decrease the hydrolysis rate of the most hydrolysable species through chemical modification.<sup>13–18</sup> Such modification of metal

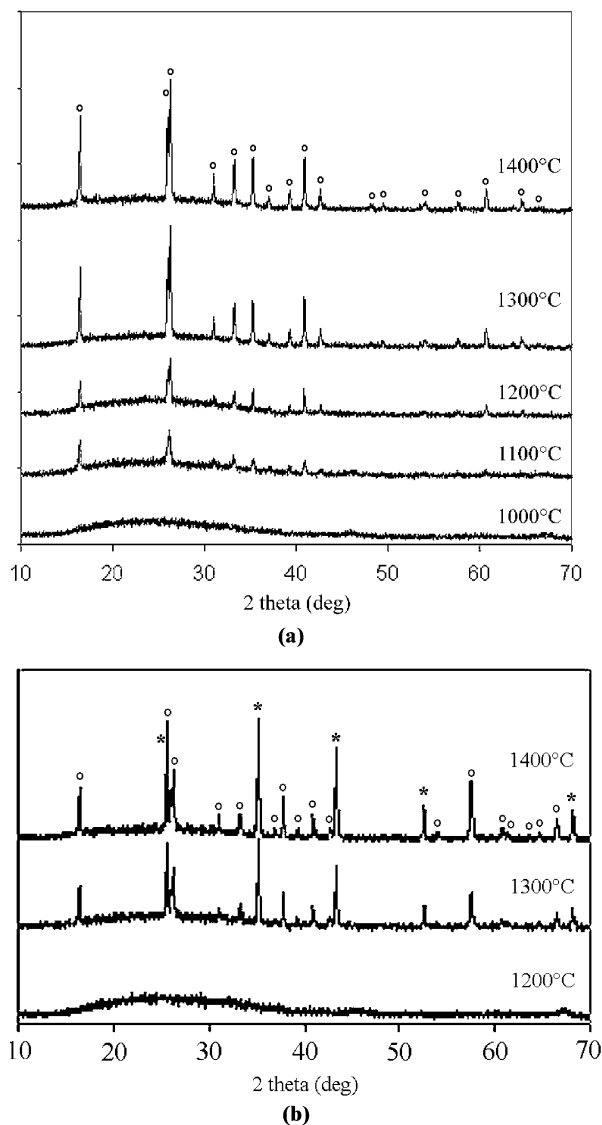


Fig. 2. X-ray diffraction patterns on the powders issued from complete hydrolysis of the precursors for samples 1 (a) and 2 (b) and heated at various temperatures (O:mullite, \*: $\alpha$ - $\text{Al}_2\text{O}_3$ ).

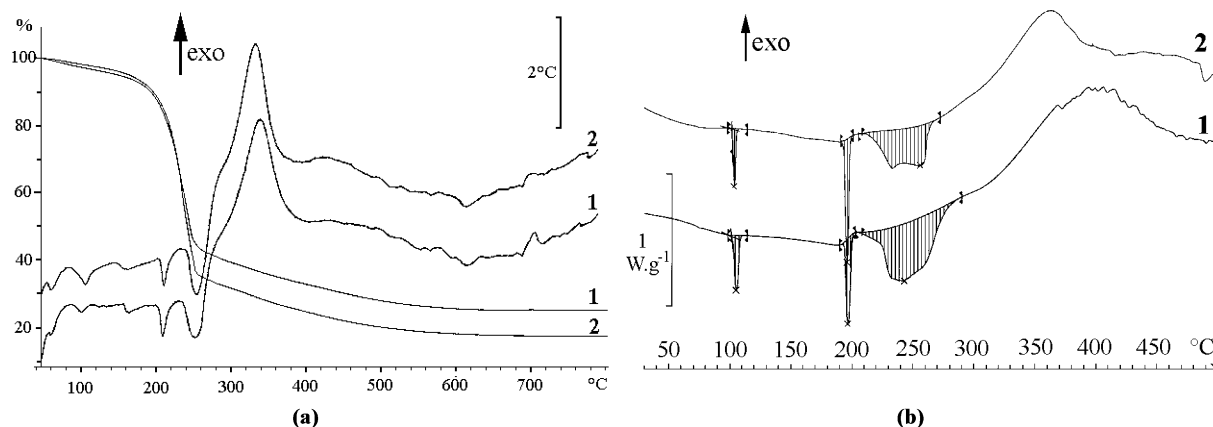


Fig. 3. TGA/SDTA (a) and DSC (b) for samples 1 and 2.

alkoxides was recently reviewed by Turova and co-workers.<sup>13</sup> Acetylacetone was used as chelating agent to stabilize the aluminium precursor and to prevent precipitation. The best results were obtained with a molar ratio  $\text{Al}(\text{OR})_3:\text{acacH} = 1:1$ .

A cationic surfactant (CTAB) was used to create the mesoporosity in the inorganic network. Self assembly of the surfactant due to electrostatic interactions with the inorganic precursors allow the formation of rod-like micelles.<sup>20–23</sup> Association of the cationic head of the surfactant with anionic aluminosilicates lead to lamellar phase which tend to form hexagonal mesophase as polymerisation of the silicates proceeds. Further elimination of the surfactant during thermal annealing generates the porosity in the inorganic network.

### 3.2. Characterization of the powders

X-ray diffraction (XRD), thermal (TGA, SDTA, DSC) and thermo-mechanical (TMA) analysis were performed on the powders issued from the complete hydrolysis of the solution. The results of the X-ray diffraction experiments are presented in the Fig. 2. The sample 1 (Fig. 2a) started to crystallise between 1000 and 1100 °C, in the pure mullite  $\text{Al}_6\text{Si}_2\text{O}_{13}$  phase. Crystallisation for the sample 2 (Fig. 2b) started higher, between 1200 and 1300 °C. The main phase was the  $\alpha$ - $\text{Al}_2\text{O}_3$  (corundum) and the secondary phase appeared to be the mullite. TGA and DSC were performed to investigate the behavior during the thermal treatments. TGA and DSC analysis performed on samples 1 and 2 showed approximately the same behavior with the precursors complete decomposition in the same temperature range (Fig. 3a,b).

The TGA (Fig. 3a) showed complete elimination of the organics between 100 and 600 °C with about 70–80% loss of mass. The DSC results (Fig. 3b) showed the endothermic melting point of the CTAB at 100 °C followed by the melting point of the aluminium acetyl-

acetate  $\text{Al}(\text{acac})_3$  at 194 °C. Decomposition of the precursors occurred at about 210 °C.

However, looking closely to the results one can see that the DSC curve for sample **1** showed a broad peak at 250 °C, which was spread over a larger range of temperature than sample **2**. SDTA results were consistent with this observation, with an endothermic signal at 230 °C, corresponding to the inflexion point of the loss of mass observed in TGA.

An exothermic reaction ( $\Delta H = 300 \text{ J g}^{-1}$ ) was observed in the range 300–500 °C for **1** and 300–400 °C for **2** corresponding to an oxidation of the latest organic residues. One can also notice on the DSC or SDTA curves that the broad exothermic peak following the endothermic phenomena was shifted towards the higher temperature for sample **1** (up to 500 °C) than for sample **2**.

The surface areas were estimated by the BET method and the results are reported in Fig. 4. The surface area was relatively high for both systems, even at high temperatures (800 °C). Some differences can be noticed between the two samples. The sample **1** (mullite) showed that the surface area increased between 400 and 600 °C with a maximum of  $510 \text{ m}^2 \text{ g}^{-1}$ , while the maximum of  $540 \text{ m}^2 \text{ g}^{-1}$  was reached at 400 °C for the sample **2** ( $\text{Al}_2\text{O}_3$ /mullite). The explanation could be that the organics were completely removed from the pores earlier for sample **2** (400 °C) than for sample **1** (600 °C). For both systems the surface area remained high at 800 °C ( $310\text{--}370 \text{ m}^2 \text{ g}^{-1}$ ) and even at 1000 °C for the oxides mixture **2** ( $170 \text{ m}^2 \text{ g}^{-1}$ ). Above 1000 °C and 1200 °C for, respectively, **1** and **2**, the surface decreased drastically due to the crystallization of the respective oxides as shown by powder X-ray diffraction and by the exothermic drift starting at 650 °C in the SDTA. The surface area decreased less rapidly for **2** because of the highest crystallization temperature of alumina.

The thermo-mechanical analysis (TMA) was used to investigate the mechanical behavior as a function of the

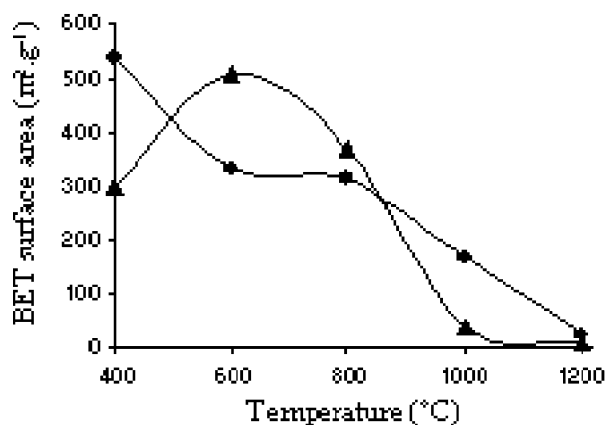


Fig. 4. Surface area (BET) for both samples **1** (▲) and **2** (●) depending on the temperature.

temperature (Fig. 5). The results were very similar for both samples. They showed a swell which was due to the formation and evolving of the gas phase during the decomposition of the organics around 250–300 °C. Then, a contraction was observed for the two samples (10–16% linear for, respectively, samples **1** and **2**). The density of the residues was compatible with a very high porous volume, which was consistent with the SEM characterization. Above 800 °C, mainly closed macropores were evidenced, with almost no contribution to the surface area.

### 3.3. Characterization of the coatings

The coatings elaborated on the fibres in our conditions were usually adherent and crack-free. The thicknesses were in the range 0.5–1  $\mu\text{m}$  depending on the dipping parameters. Cracks were observed when rapid thermal annealing (300–500 °C) was applied. Therefore drying at 120 °C between the layers and thermal annealing with a rate of 5 °C/min were performed on the samples to prevent cracking. The SEM characterisations are presented on the  $3\text{Al}_2\text{O}_3\text{--}2\text{SiO}_2$  composition (**1**) but similar results were observed with the oxides mixture (**2**). Figs. 6 and 7 show typical scanning electron micrograph for the Al–Si–O coatings. The surface was very homogeneous and smooth, without apparent defect (Fig. 6a). For a fibre annealed at 500 °C in the air, the distribution of the mesopores at the surface looked very regular, and the size of the mesopores (50 nm) was nearly monodisperse (Fig. 6b). The observation of the cross-section of a fibre annealed at 1200 °C for 1 h in the air showed that the oxide particles size was 50 nm (Fig. 7a,b). The pore distribution evidenced on the surface of this fibre was much less homogeneous with sizes of about 100–200 nm (Fig. 7c).

The thicknesses of the coatings were estimated either directly from scanning electron micrographs on the fibres cross-sections or using laser interferometer. As previously mentioned,<sup>6</sup> the dipping time was one of the most influential parameters on the thickness of the films. Usually the thickness  $\lambda$  of the film can be correlated to the withdrawal

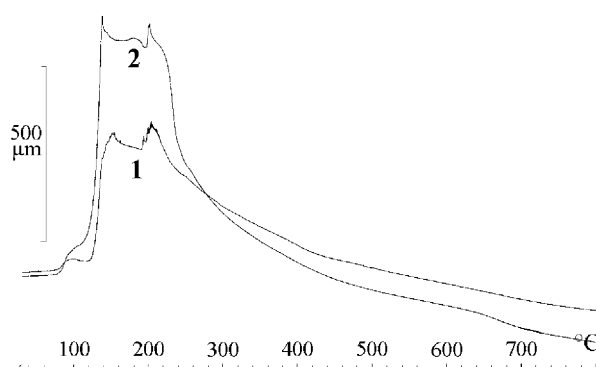


Fig. 5. Thermomechanical analysis for samples **1** and **2**.



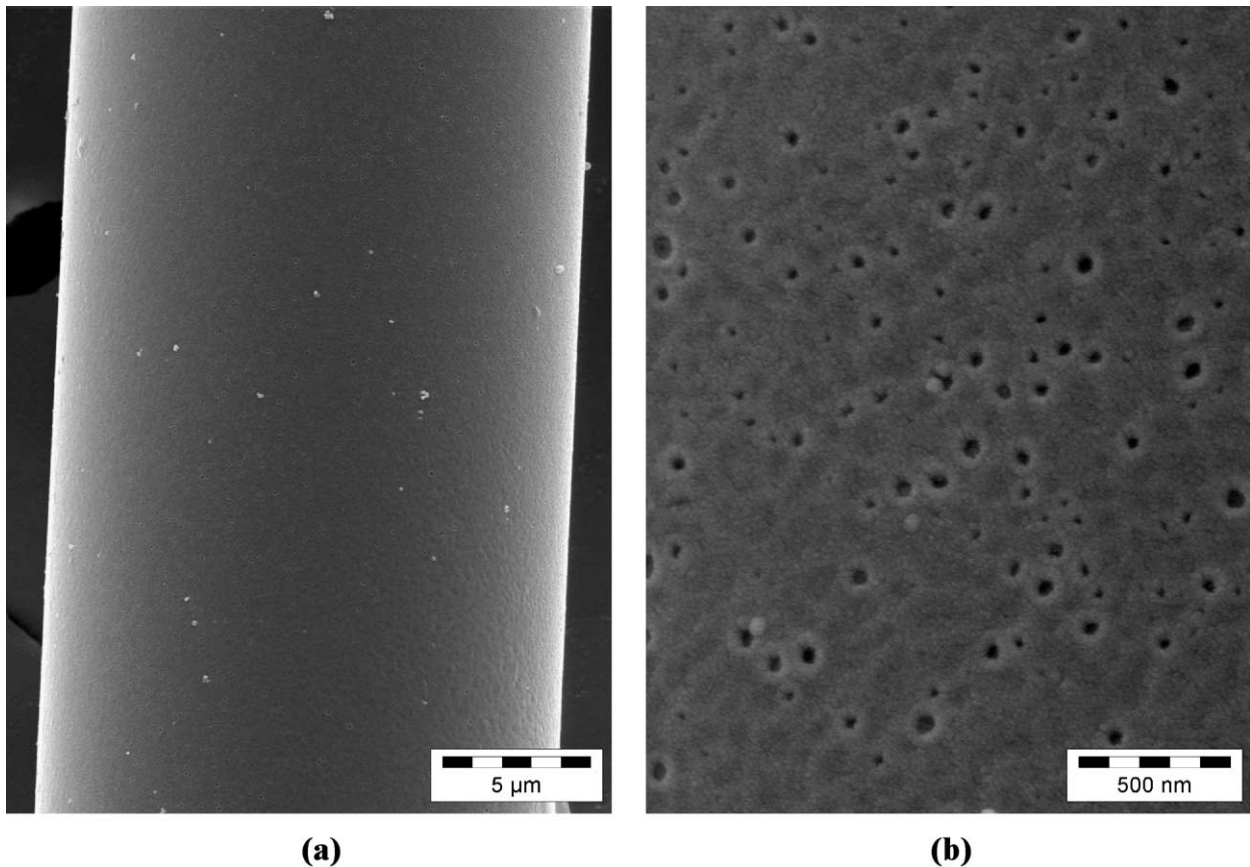


Fig. 6. Scanning electron micrographs of the surface of the coated fibres annealed at 500 °C.

speed  $v$ , the density  $\rho$  and the viscosity  $\eta$  of the sols following Eq. (1), where  $g$  is the gravity acceleration ( $9.806 \text{ m}\cdot\text{s}^{-2}$ ) and  $k$  is a correction factor ( $k=0.1$ ).<sup>12</sup>

$$\lambda = k[(\eta \cdot v)/(\rho \cdot g)]^{1/2} \quad (1)$$

This was demonstrated mainly on macroscopic substrates. In our case the substrates were microscopic, with a particular shape (fibre). Theoretical and few experimental works were previously reported concerning deposition on microscopic fibres taking into account the diameter of the fibre and the surface tension of the solvent which become much more influential than at the macroscopic level.<sup>9,24</sup> In any case it has been shown that the experimental values do not fit with the predicted ones. The evolution of the viscosity of the alkoxides solution could explain this difference. Another parameter that could be considered is the chemical reactivity of the sol and/or the precursors at the surface of the substrate. However, this hypothesis would necessitate some further investigations.

### 3.4. Characterization of the mechanical behaviour

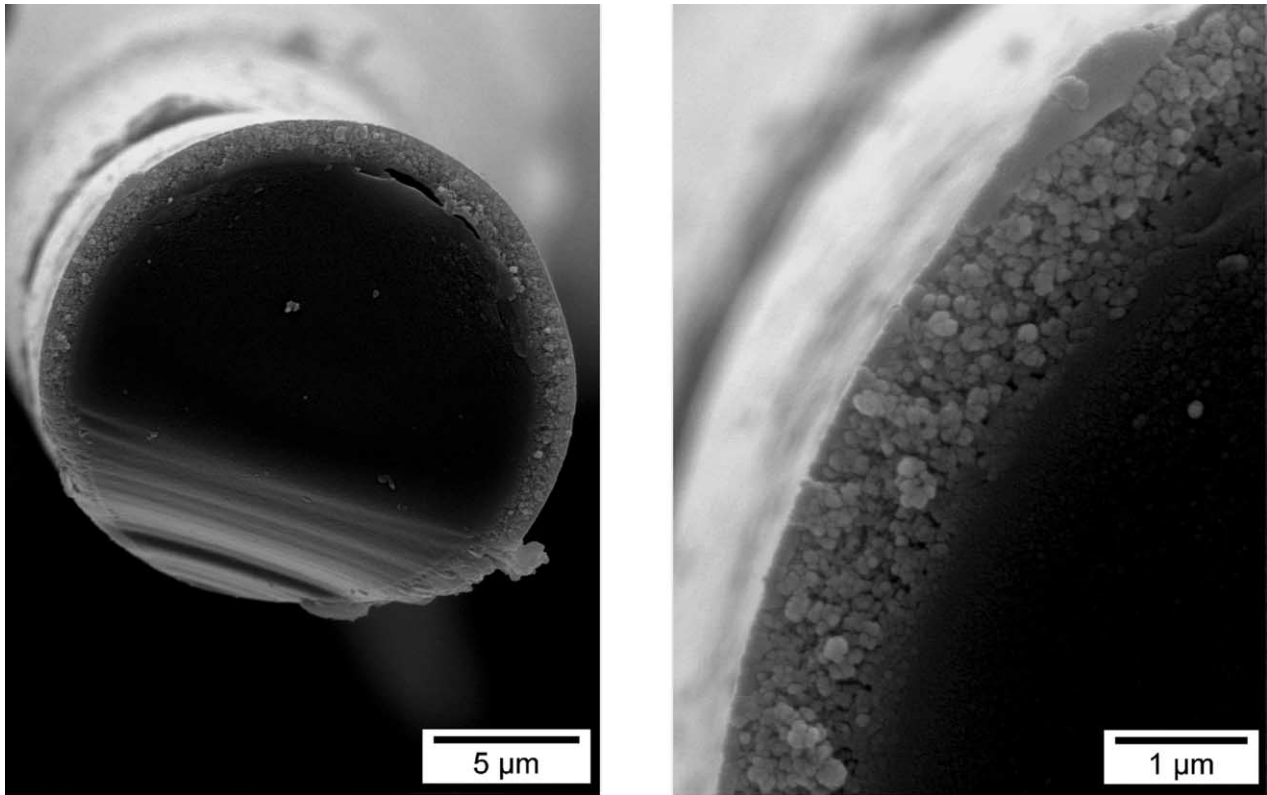
Table 2 summarizes the thermo-mechanical properties measured on the commercial SiC Hi-Nicalon fibres.

Hi-Nicalon fibres, coated with a 0.5 µm film with both systems and uncoated fibres, treated at 600 and 1200 °C for 1 h in air were tensile tested. Results are reported in Table 3. The tensile strength fell drastically down for a fibre treated at 1200 °C in the air (2170 MPa) while it was maintained relatively high for a fibre coated with the oxide (2970 MPa) compared to the results obtained on the commercial fibre (3000 MPa). The tensile modulus of the coated fibres after thermal annealing at 1200 °C (270 GPa) was very similar to the commercial fibres (270 GPa) while it was lower for the uncoated fibres (230 GPa). These observations evidenced the protective role of the coatings towards oxidation reactions.

Table 2

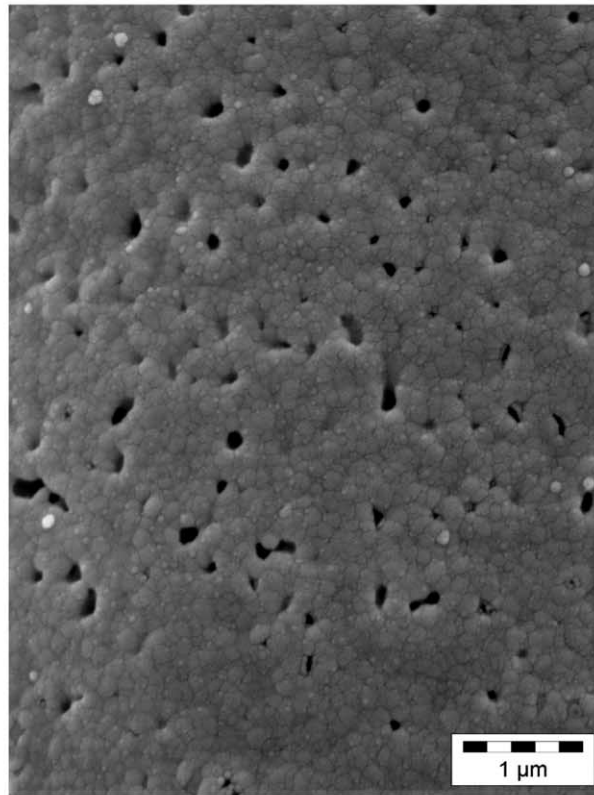
Experimental mechanical properties of the commercial Hi-Nicalon SiC fibres

Properties	Hi-Nicalon fibre
Fibre diameter (µm)	14
Tensile modulus (GPa)	270
Tensile strength (MPa)	3000
Density ( $\text{g cm}^{-3}$ )	2.74
Elongation (%)	1.1
Thermal expansion coefficient ( $^{\circ}\text{C}^{-1}$ )	$4.6 \times 10^{-6}$



(a)

(b)



(c)

Fig. 7. Scanning electron micrographs of the cross-section (a, b) and the surface (c) of the coated fibres annealed at 1200 °C in the air.

Table 3  
Tensile tests on the coated SiC fibres for systems 1 and 2 after annealing at 600 and 1200 °C

	SiC Hi-Nicalon	Hi-Nicalon treated at 1200 °C in air	Coated Hi-Nicalon treated at 1200 °C in air
Tensile strength (MPa)	3000	2170	2970
Tensile modulus (GPa)	270	230	270
Weibull modulus	6.9	5.5	4.8

The original mechanical properties were preserved after the deposition of the oxide. Moreover, at high temperatures in an oxidative atmosphere, the mechanical behaviours were much better with a coated fibre than with the uncoated ones.

#### 4. Conclusion

Thin films of mixed silicon/aluminium oxides on SiC Hi-Nicalon fibres were successfully elaborated using the sol-gel process. The coated fibres were stable in an oxidative environment even at high temperatures (1200 °C). The protective role of the oxides was thus demonstrated, as well as the good mechanical behavior of the fibre/coating system. These porous coatings are therefore potential interphases for applications in Ceramic Matrix Composites and micro-composites SiC/Oxide/SiC which are currently under investigation.

#### Acknowledgements

The authors wish to thank the CNRS for financial support.

#### References

- Carpenter, H. W. and Bohlen, J. W., Fibers coatings for ceramic matrix composites. *Ceram. Eng. Sci. Proc.*, 1992, **13**(7–8), 238–256. H.W. Carpenter, J. Bohlen and N.S. Steffier, Weak frangible fiber coating with unfilled pores for toughening ceramic fiber-matrix composites, US Patent No. 5,221,578, 1992.
- Reig, P., Demazeau, G. and Naslain, R.,  $\text{KMg}_2\text{AlSi}_4\text{O}_{12}$  phyllosiloxide as potential interphase material for ceramic matrix composites. *J. Mater. Sci.*, 1997, **32**, 4195–4200.
- Tressler, R. E., Recent developments in fibers and interphases for high temperature ceramic matrix composites. *Composites: Part A*, 1999, **30**, 429–437.
- Cinibulk, M. K. and Hay, R. S., Textured magnetoplumbite fiber-matrix interphase derived from sol-gel fiber coatings. *J. Am. Ceram. Soc.*, 1996, **79**(5), 1233–1246.
- Wurm, R., Dernovsek, O. and Greil, P., Sol-gel derived  $\text{SrTiO}_3$  and  $\text{SrZrO}_3$  coatings on SiC and C-fibers. *J. Mater. Sci.*, 1999, **34**, 4031–4037.
- Parola, S., Verdenelli, M., Sigala, C., Scharff, J.P., Velez, K., Veytizou, C., and Quinson, J.F. Sol-gel coatings on non-oxide planar substrates and fibers: a protection barrier against oxidation and corrosion. *J. Sol-Gel Sci. Tech.* (in press).
- Hashishin, T., Murashita, J., Joyama, A. and Kaneko, Y., Oxidation-resistant coating of carbon fibers with  $\text{TiO}_2$  by sol-gel method. *J. Ceram. Soc. Jap. Int. Ed.*, 1998, **106**, 4–8.
- Aparicio, M. and Durán, A., Yttrium silicate coatings for oxidation protection of carbon-silicon carbide composites. *J. Am. Ceram. Soc.*, 2000, **83**(6), 1351–1355.
- Gundel, D. B., Taylor, P. J. and Wawner, F. E., Fabrication of thin oxide coatings on ceramic fibres by a sol-gel technique. *J. Mater. Sci.*, 1994, **29**, 1795–1800.
- Karlin, S. and Colomban, Ph., Micro-Raman study of SiC fibre-oxide matrix reaction. *Composites Part B*, 1998, **29B**, 41–50.
- Colomban, Ph., Bruneton, E., Lagrange, J. L. and Mouchon, E., Sol-gel mullite matrix-SiC and-mullite 2D woven fabric composites interphase: elaboration and properties. *J. Eur. Ceram. Soc.*, 1996, **16**, 301–314.
- Brinker, C. J. and Scherer, G. W., *Sol-Gel Science: The Physics and Chemistry of Sol-Gel Processing*. Academic Press, San Diego, 1990.
- Turova, N.Ya., Turevskaya, E. P., Kessler, V. G. and Yanovskaya, M. I., *The Chemistry of Metal Alkoxides*. Kluwer Academic Publishers, Norwell MA, 2001.
- Bradley, D. C., Mehrotra, R. C. and Gaur, D. P., *Metal Alkoxides*. Academic Press, London, 1978.
- Sanchez, C., Livage, J., Henry, M. and Babonneau, F., Chemical modification of alkoxide precursors. *J. Non-Cryst. Solids*, 1988, **100**, 65–76.
- Verdenelli, M., Parola, S., Hubert-Pfalzgraf, L. G. and Lecocq, S., Tin dioxide thin films from Sn(IV) modified alkoxides—synthesis and structural characterization of  $\text{Sn}(\text{OEt})_2(\text{acac})_2$  and  $\text{Sn}_4(\text{O})_2(\text{OEt})_{10}(\text{acac})_2$ . *Polyhedron*, 2000, **10**, 2069–2075.
- Velez, K., Quinson, J. F. and Fenet, B., Modification study of aluminium sec-butoxide by acrylic acid. *J. Sol-gel Sci. Technol.*, 1999, **16**, 201–208.
- Nass, R. and Schmidt, H., Synthesis of an alumina coating from chelated aluminium alkoxides. *J. Non-Cryst. Solids*, 1990, **121**, 329–333.
- Patankar, S. N., Weibull distribution as applied to ceramic fibres. *J. Mater. Sci. Let.*, 1991, **10**, 1176–1181.
- Kresge, C. T., Leonowicz, M. E., Roth, W. J., Vartuli, J. C. and Beck, J. S., Ordered mesoporous molecular sieves by a liquid-crystal template mechanism. *Nature*, 1992, **359**, 710–712.
- Monnier, A., Schüth, F., Huo, Q., Kumar, D., Margolese, D., Maxwell, R. S., Stucky, G. D., Krishnamurty, M., Petroff, P., Firouzi, A., Janicke, M. and Chmelka, B. F., Cooperative formation of inorganic-organic interfaces in the synthesis of silicate mesostructures. *Science*, 1993, **261**, 1299–1303.
- Murakata, T., Sato, S., Ohgawara, T., Watanabe, T. and Suzuki, T., Control of pore size distribution of silica gel through sol-gel process using inorganic salts, surfactants as additives. *J. Mater. Sci.*, 1992, **27**, 1567–1574.
- Zhou, H. S., Kundu, D. and Honma, I., Synthesis of oriented meso-structure silica functional thin film. *J. Eur. Ceram. Soc.*, 1999, **19**, 1361–1364.
- Goucher, F. S. and Ward, H., A problem in viscosity: the thickness of liquid films formed on solid surfaces under dynamic conditions. *Phil. Mag. 6th Ser.*, 1922, **44**, 1002–1014.